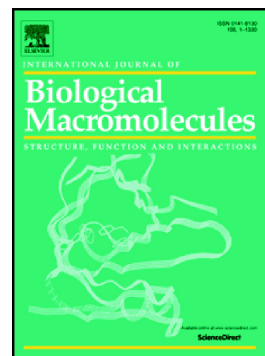


Licochalcone A loaded multifunctional chitosan hyaluronic acid hydrogel with antibacterial and inflammatory regulating effects to promote wound healing

Zhiquan Hou, Yahong Wang, Siqi Chen, Zhonghua Luo, Yunen Liu



PII: S0141-8130(24)08267-9

DOI: <https://doi.org/10.1016/j.ijbiomac.2024.137458>

Reference: BIOMAC 137458

To appear in: *International Journal of Biological Macromolecules*

Received date: 19 August 2024

Revised date: 17 October 2024

Accepted date: 8 November 2024

Please cite this article as: Z. Hou, Y. Wang, S. Chen, et al., Licochalcone A loaded multifunctional chitosan hyaluronic acid hydrogel with antibacterial and inflammatory regulating effects to promote wound healing, *International Journal of Biological Macromolecules* (2024), <https://doi.org/10.1016/j.ijbiomac.2024.137458>

This is a PDF file of an article that has undergone enhancements after acceptance, such as the addition of a cover page and metadata, and formatting for readability, but it is not yet the definitive version of record. This version will undergo additional copyediting, typesetting and review before it is published in its final form, but we are providing this version to give early visibility of the article. Please note that, during the production process, errors may be discovered which could affect the content, and all legal disclaimers that apply to the journal pertain.

Licochalcone A loaded multifunctional chitosan hyaluronic acid hydrogel with antibacterial and inflammatory regulating effects to promote wound healing

Zhiquan Hou^{a,†}, Yahong Wang^{a,†}, Siqi Chen^b, Zhonghua Luo^{c*}, Yunen Liu^{c*}

^a*Graduate School, Shenyang Medical College, No. 146, Huanghe North Street, Shenyang 110034, China*

^b*School of Public Health, Shenyang Medical College, No. 146, Huanghe North Street, Shenyang 110034, China*

^c*Shuren International College, Shenyang Medical College, No. 146, Huanghe North Street, Shenyang 110034, China*

*Corresponding author: Zhonghua Luo, Ph.D; Prof. Yunen Liu, Ph.D

Phone: +86-024-62215130; E-mail: liuye990116@163.com

Phone: +86-024-62215131; E-mail: zhonghua_2398@163.com

† These authors contributed equally to this work.

Abstract: The wound healing process is characterized by persistent infection and long-term inflammation. The licochalcone A (LicA) has the potential for skin wound healing and needs a good drug-loading platform to apply its antibacterial and anti-inflammatory effects. In this study, the LicA@chitosan (CS) -hyaluronic acid (HA) hydrogel with antibacterial and anti-inflammatory was developed for wound healing in mice. The SEM displayed that the hydrogel had an obvious porous structure and was very suitable to be used as a delivery carrier for LicA. The FTIR results suggested that the LicA can be effectively loaded in the CS-HA hydrogel. Variable strain scanning, frequency scanning and temperature scanning indicated that the LicA@CS-HA hydrogel can maintain the gel state. The LicA@CS-HA hydrogel had good biological safety, can inhibit the activity of *Escherichia coli* and *Staphylococcus aureus*, and can release LicA stably. The LicA@CS-HA hydrogel also has good adhesion and hemostatic properties. Finally, the LicA@CS-HA hydrogel significantly accelerated wound healing in mice skin injury model, and reduced inflammation and orderly collagen deposition were observed by HE and Masson staining. The immunohistochemistry indicated that the LicA@CS-HA hydrogel induced the positive expression of CD31, VEGF, and HIF-1 α promoted neovascularization. The LicA@CS-HA hydrogel also down-regulated the expression of M1 macrophage markers CD86, IL-6, and TNF- α , and increased the expression of M2 macrophage markers CD206, IL-4, and IL-10 proteins. The molecular docking demonstrated that the target proteins had better binding activity to LicA. Collectively, the LicA@CS-HA hydrogel has broad application prospects in promoting wound healing.

Keywords: LicA@CS-HA hydrogel; Wound healing; Macrophage polarization; Angiogenesis; Molecular docking

1. Introduction

The skin is an important and effective protective barrier against changes in the external environment. When the skin is injured to form a wound, the body produces a lot of complicated processes to re-establish this protection. Wound healing usually takes place in four phases: the coagulation phase, the inflammatory phase, the proliferation phase, and the maturation phase. Persistent periods of inflammation are a prominent pathophysiological feature, causing difficulty in wound healing and the potential for infection. However, the dysfunction of macrophages with dysregulated expression and excessive release of pro-inflammatory factors are thought to be the main reasons [1-3]. Studies have presented that wound healing is closely related to the phenotypic shift from pro-inflammatory to anti-inflammatory macrophages. Macrophages play a critical role in the coordination of the transition between the four stages of wound healing [1,4]. However, therapeutic approaches to modulate macrophage expression and improve the inflammatory response to wounds remain scarce and do not achieve the desired results. Therefore, it is vital to design and develop effective treatments to improve macrophage expression during wound healing and reduce wound inflammation.

In recent years, traditional Chinese medicine has attracted much attention for its unique therapeutic effects in the process of wound healing [5]. Promoting wound healing and anti-inflammation and antibacterial are the important standards of traditional Chinese medicine in wound treatment [6]. Licorice is one of the earliest discovered and most popular medicinal herbs since ancient times and is well documented in the pharmacopeias of China as well as Western countries [7]. As a traditional Chinese medicine, licorice is known for its heat-clearing, detoxifying, and anti-inflammatory properties [7-9]. Furthermore, licorice has applications in the manufacturing and light industry, including the preparation of cosmetics, soaps, and oral health products [10,11]. Licorice extract is as well as widely used in the food industry. For example, glycyrrhizin is one of the natural sweeteners currently used to adjust the taste of healthy foods, and glycyrrhizic acid is used as a foaming agent in foods such as wine, alcoholic beverages, confectionery, and sweets [12]. Licochalcone A (LicA) is one of the flavonoids extracted from licorice, which has potent anti-inflammatory, antibacterial, and antioxidant properties, and participates in the immune regulation of the human body [13,14]. According to the literature, LicA

can inhibit the expression of pro-inflammatory mediators such as tumor necrosis factor (TNF- α), interleukin (IL)-6, and IL-1 β [15, 16]. However, the poor bioavailability of LicA limits its application [13].

It has been reported that hydrogel dressings have a three-dimensional porous structure and high porosity, which is an effective carrier for loading bioactive substances to improve drug utilization [17-19]. Chitosan (CS) and hyaluronic acid (HA), as common natural polymers, are often used in bioengineered skin substitutes, bioscaffolds, drug carriers, and biological dressings [20]. The CS is the product obtained from the deacetylation of chitin, which is the only alkaline polysaccharide found in nature. It is rich in sources and can be used as a hydrogel dressing with the functions of hemostasis, biodegradability, anti-inflammation, and antibacterial [21,22]. Additionally, the CS is degradable, and its good biocompatibility gives it a good physical barrier capability [23]. The HA is a mucopolysaccharide component of the extracellular matrix (ECM) that promotes cell adhesion, proliferation, and differentiation, and is highly hydrophilic, which makes it an ideal candidate for the preparation of wound dressings [24,25]. However, traditional single-component hydrogels are poorly biocompatible and lack the orderly and dynamic structure of biological soft tissues, and the overall therapeutic effect is not well [26]. In order to satisfy the need for wound healing, the development of new multifunctional hydrogel dressings with excellent anti-inflammatory and antibacterial properties, self-healing properties, loadability, and excellent biocompatibility have become an important direction of research [27].

Therefore, in this study, we combined the CS and the HA by physical crosslinking method to prepare a safe, effective, and mechanically stable multifunctional polymer hydrogel dressing for regulating wound inflammation and promoting wound tissue regeneration. Based on the pharmacological effects of LicA and the biological characteristics of the CS-HA hydrogel, the LicA@CS-HA hydrogel was designed to improve the bioavailability of LicA in vitro and in vivo, improve wound inflammation and promote wound healing. The physical properties, safety, antibacterial properties, and hemostatic properties of the LicA@CS-HA hydrogel were studied. The effect of the LicA@CS-HA hydrogel in promoting wound healing were studied by animal experiments. Meanwhile, molecular docking results strongly verify the binding ability of LicA to target proteins. In conclusion, the LicA@CS-HA hydrogel provides new insight for developing wound healing therapy.

2. Materials and methods

2.1 Material

The CS (mean molecular weight (Mw) of 62×10^4 and the HA (molecular weight, 1500-2500 kDa) were purchased from China Pharmaceutical Group Chemical Reagent Co. The MEM medium (XP0034) was supplied by Shanghai Darthel Biotechnology Co. The cell Counting kit-8 (CCK8) (CA1210) was provided by Beijing Soleberg Technology Co. The L929 cell line (mouse fibroblast) (CL-0137) and 10% Fetal Bovine Serum (FBS) (164210-50) were obtained from Wuhan Purcellino Technology Co. The LB agar plates (HBPM0129) were purchased from Haibo Biotechnology Co. The bicinchoninic acid (BCA) (FD2001) detection kits were bought from Fdbio Science Biotech Co., Ltd. The TNF- α (#11948) was supplied by Cell Signaling Technology Co. The IL-6 (ab7737), IL-4 (ab9728), IL-10 (ab9969), and CD31 (ab28364) were purchased from Abcam Trading Co. The CD86 (00111743) and CD206 (00126512) were sourced from Proteintech Biotech. The LicA (purity $\geq 95\%$) was self-made according to the method of Luo et al [28].

2.2 Preparation and characterization of the CS-HA hydrogel and LicA@CS-HA hydrogel

The 2.9 g of CS powder and 30 g of saline were mixed and stirred, then 0.8 g of glacial acetic acid solution (0.5% W/V) was added and stirred at room temperature. When the gel state appeared, 3 g of the HA powder was added and stirred continuously to obtain the CS-HA hydrogel. After obtaining the hydrogel in the same way as described above, 185 mg of LicA powder (5 mg/mL) dissolved by ultrasonic oscillation was added to obtain the LicA@CS-HA hydrogel.

2.3 Characterization of the CS-HA hydrogel

2.3.1 Characterization of the CS-HA hydrogel by Infrared spectrum

The infrared spectra of LicA, the CS-HA hydrogel, and the LicA@CS-HA hydrogel were tested by FTIR (Tensor 27, Bruker, Billerica, USA) with wave number scans ranging from 500 cm^{-1} -4000 cm^{-1} .

2.3.2 Scanning electron microscope (SEM) of the CS-HA hydrogel

The internal structure of the LicA@CS-HA hydrogel was observed by SEM (QUANTA 450, FEI, USA). The gel sample was freeze-dried for 24 h, and the freeze-dried hydrogel sample was cut and attached to the metal table with a relatively flat surface facing outward after gold-spraying

treatment, and then placed under SEM for observation and photography.

2.3.3 Drug release analysis of LicA

The release of LicA was analyzed by a UV-visible NIR spectrophotometer. 5 mg of LicA was precisely weighed and dissolved in 20 mL of PBS buffer with 0.5% Tween 80 and stored away from light. Afterwards, the UV absorption spectrogram of LicA at 200-800 nm was tested to determine the wavelength of the maximum peak. The samples were immersed in PBS buffer and 2 mL of the immersion solution was removed at different times to test the absorbance at 420 nm, then 2 mL of PBS buffer was added to the immersion solution.

2.3.4 Tensile strength test

The tensile mechanical properties of hydrogel samples were investigated by a universal materials testing machine equipped with a 1 kN transducer. The hydrogel samples were cut into dumbbell-shaped specimens (2 mm wide \times 10 mm long \times 1.5 mm thick) for tensile testing, and the tensile strength and elongation at break were determined. The tensile speed was set to 100 mm/min.

2.3.5 Rheological analysis

The rheological properties of hydrogel were tested by rheometer (MARS 60), and the changes of storage modulus (G') and loss modulus (G'') were recorded by variable strain scan in the scanning range of 1% -1000%. Frequency scanning was used to observe the changes of G' and G'' between 1 Hz and 100 Hz. The changes of G' and G'' were recorded by temperature scanning from 0°C to 50°C, in which the strain was 1% and the frequency was 1 Hz.

2.3.6 Mechanical performance test

The mechanical properties of hydrogel samples of the same size were measured using the MT480 universal mechanical tester produced by Shenzhen Meister. The hydrogel samples were prepared into cylindrical shapes (12 mm height \times 15 mm diameter) for compression testing. The compression tests were carried out at room temperature with a compression rate of 2 mm/min and compressive strains of 59% and 69%, respectively. Each hydrogel sample was tested more than five times and the average value was taken.

2.4 In vivo degradation of the the hydrogel

The experimental animals and protocol have been approved by the Animal Protection and Ethics Committee of Shenyang Medical College (SYYXY2023092001). The rats were

anesthetized with 1.5% isoflurane and implanted with a hydrogel under the skin of the back. 7 days and 14 days after implantation, the tissue implanted with the hydrogel was obtained. HE staining was performed to determine the inflammatory response (n=3). The stained tissue was then observed.

2.5 *In vitro* antimicrobial assay

The *Escherichia coli* (*E. coli*) and *Staphylococcus aureus* (*S. aureus*) were used to assess the antimicrobial activity of the LicA@CS-HA hydrogel. Briefly, the bacteria were revived and passaged to prepare bacterial suspensions, and then the concentration of bacterial suspensions was measured using a turbidimeter, which was about $1\sim 2\times 10^8$ CFU/mL. The *E. coli* and *S. aureus* were divided into four groups, respectively. The bacterial suspensions were added to each experimental group, incubated in the incubator at 37°C for 2 h, and then resuspended in 1 mL of sterile PBS buffer. Next, the resuspension was evenly applied in the bacterial petri dishes, which were put into the incubator for 24 h. Finally, observation and photographs were taken. The bacterial sterilization rate was given by the following formula.

$$\text{Sterilization rate (\%)} = \frac{(\text{number of bacteria in control group} - \text{number of bacteria in drug group}) \times 100\%}{(\text{number of bacteria in control group})}$$

2.6 Cytotoxicity assay

The cytotoxicity of the materials in L929 cells was assessed using the CCK8 assay. The L929 cells were inoculated in 96-well plates at a cell density of 5×10^4 cells/well, and after 24 h of incubation, the blank group was the zero-regulated wells, the normal containing cell suspension was used as the control group, and 10 μ L of the material extract was added to the experimental groups, respectively. The incubation was continued for 24 h. 100 μ L of fresh medium were added to each well after discarding the original medium. Then 10 μ L of CCK8 solution were added to each well and after incubation for 4 h. The absorbance was read by an enzyme-labeled instrument. The viability of the cells was given by the following announcement.

$$\text{Cell viability of each group (\%)} = \frac{(\text{OD value of experimental group} - \text{OD value of zero - adjustment group})}{(\text{OD value of control group} - \text{OD value of zero adjustment group})} \times 100\%$$

2.7 Cell scratching assay

The L929 cells were inoculated into 6-well plates at a density of 5×10^5 per well and cultured for 24 h. A straight line was scratched vertically in the middle area of each well with a 200 μ L

lance tip. Each well was then filled with the material extract separately and the wells without drug intervention were set as the control. Changes in the scratched area of each group were observed via a microscope, and photographs were taken at 0 and 24 h, respectively. The scratch area of each group at 0 and 24 h was measured by Image-J software.

2.8 Adhesion experiment of the LicA@CS-HA hydrogel

The C57BL/6 male mice, weighing 22-25 g, aged 8-10 weeks, were reared at room temperature for one week. This study was approved by Laboratory Animal Ethics Committee of Shenyang Medical College (SYYXY2023021501). The mice were anesthetized with isoflurane at a concentration of 1% to 1.5%. The prepared LicA@CS-HA hydrogel was used to adhere different organs of mice, including heart, spleen, lung and skin. The adhesive properties of the LicA@CS-HA hydrogel

2.9 Hemostasis test

The male sprague-dawley rats (220-250 g) were kept at room temperature and operated after 7 days of adaptation. The animals were kept in the Laboratory Animal Center of Shenyang Medical College, and the animal experiment process and operation were reviewed and approved by the Laboratory Animal Ethics Committee of Shenyang Medical College (SYYXY2023032001).

The rats were anesthetized with isoflurane at a concentration of 2% to 3%, and the tail was cut with surgical scissors from the base of the tail up to 6 cm. The control group and the LicA@CS-HA hydrogel intervention group were set up, and the tail of rats was placed on white filter paper weighed in advance. Bleeding in the tail at 3 min and 5 min was observed, and the weight of the filter paper was measured.

2.10 Establishment of mice model

All animal experiments were conducted by the European regulations on the care and use of animals in experimental procedures, and the use of laboratory animals was approved by the laboratory of the Experimental Animal Research Centre of Shenyang Medical College (SYYXY2023033001). Forty-eight C57BL/6 male mice, weighing 22-25 g, 8 to 10 weeks, were provided by Henan Scopes Bio-technology Co. The mice were acclimatized and fed for 7 days before surgery, and the ability of the LicA@CS-HA hydrogel to promote wound healing was assessed by establishing a full skin defect wound. These mice were randomly divided into the

control group, the LicA group, the CS-HA hydrogel group and the LicA@CS-HA hydrogel group, n=12. The pharmacological interventions were administered to the mice on the first three postoperative days, and trauma photographs were taken on the days 0, 3, 5, 7, 9, and 11 with a camera at the same height and angle for each mouse. The trauma area was measured and analyzed using Image-J software to calculate the trauma healing rate.

2.11 Histological analysis

On the 7th and 14th day of the experiment, wound skin tissues were fixed in 4% paraformaldehyde for 48 h, dehydrated with conventional gradient ethanol, embedded, sliced with a thickness of 4 μm , stained with HE and Masson, and sealed with neutral resin. The sections are viewed under a microscope (Leica, DM4B) and photographed.

2.12 Immunohistochemical analysis

The tissue sections were dewaxed into water, then the antigen was repaired, primary antibody solutions (CD31, 1:100, HIF-1 α , 1:250, VEGF: 1:200) were added and incubated in the dark for 30 min. After washing with PBST, the secondary antibody solution was added and incubated at room temperature for 1 h. Then, DAB was used for color development, hematoxylin was re-dyed, and the tissue sections were dehydrated and sealed with neutral gum. The images were observed and collected under the microscope, and analyzed by Image-J software.

2.13 Immunofluorescence analysis

The tissues were sliced and dewaxed to water. After antigen repair, the primary antibodies diluted by PBST (CD86, 1:100, CD206, 1:200) were added and incubated in a constant temperature water tank for 1 h. The second antibody Alexa Fluor (R) was dripped on the sliced tissue and incubated in a constant temperature water tank for 2 h. The plates were then sealed with an anti-fluorescence quenched tablet containing DAPI, observed with a confocal laser fluorescence microscope (Zeiss LSM 800), and images were captured.

2.14 Molecular docking

The 3D eutectic structure and small molecule ligand structure of active proteins were downloaded from PDB (PDB ID of TNF- α , 1TNR. PDB ID of IL-6, 1N26, PDB ID of IL-4, 1H1K, PDB ID of IL-10, 1INR) and TCMSP databases, then saved in pdb format. The energy of CBD was minimized by Chem3D 21.0.0 software. The SYBYL-X2.0 software was used to convert the active component and target protein from pdb format to mol2 format after

hydrogenation and loading. The SYBYL-X2.0 was used to buttonize the active component, calculate the score, and analyze the visual image [29,30].

2.15 Western blotting

For western blot analysis, wound tissue proteins were extracted by using Mammalian Reagent Kits (Fubio Science Co., Ltd., Hangzhou, China). Afterward, the amount of protein was measured by the BCA kit. The protein extracts were separated by sodium dodecyl sulfate-polyacrylamide gel electrophoresis (SDS-PAGE) and transferred to polyvinylidene difluoride membranes (Immobilon P, Millipore, Billerica, USA). The membrane was sealed with 5% skim milk at room temperature for 1 h. The membrane was incubated with the primary antibody at 4°C overnight and cleaned with PBST. Then, the membranes were added with the secondary antibody, incubated at 37°C for 1 h, and cleaned with PBST. Immunoreactive bands were observed using enhanced chemiluminescence reagents (Thermo Fisher Scientific, Waltham, USA) and imaged by ChemiDoc XRS Plus luminescence image analyzer (Bio-Rad). Densitometric quantitative analysis of band intensities was performed using Image-J software.

2.16 Statistics analysis

All the statistical analyses of the experimental data were conducted with GraphPad Prism 8.0 (GraphPad, USA). The data were reported as mean \pm standard deviation (SD). The one-way ANOVA was used to determine the differences among three or more groups. $p < 0.05$ was regarded as statistically significant.

3. Results

3.1 Preparation and characterisation of the LicA@CS-HA hydrogel

In this study, we first prepared the CS-HA hydrogel, and LicA was further physically crosslinked with the CS-HA hydrogel to prepare the LicA@CS-HA hydrogel (Fig. 1A). The structural characteristics of the LicA, the CS-HA hydrogel and the LicA@CS-HA hydrogel were observed by SEM. As shown in Fig. 1B, the CS-HA hydrogel and the LicA@CS-HA hydrogel displayed typical three-dimensional porous structures, and the LicA was efficiently loaded. Subsequently, the drug release assay was carried out by UV spectrophotometry to assess the utilization of the LicA. As indicated in Fig 1C, when the LicA was loaded on the CS-HA hydrogel, it was observed that the release curve reached its peak on the 5th day, followed by a slow release with a decreasing trend. To further prove whether the LicA@CS-HA hydrogel was constructed

successfully, we verified it by FTIR spectroscopy. As suggested in Fig. 1D, the spectral results of LicA indicated that the stretching vibration absorption peak of C=O was at 1585 cm^{-1} , the stretching vibration absorption peak of C-O was at 1288 cm^{-1} , the stretching vibration absorption peak of C-O-C was at 1042 cm^{-1} , and the 832 cm^{-1} was the out-of-plane bending vibration peak of the binary aromatic cyclic hydrogen. The spectrum diagram of the CS-HA hydrogel displayed that the stretching vibration absorption peak of O-H and N-H was at 3263 cm^{-1} , and the bending vibration absorption peak of N-H was at 1538 cm^{-1} . Then, the 1151 cm^{-1} was the stretching vibration absorption peak of the C-O bond, and the 1007 cm^{-1} was the stretching vibration absorption peak of the C-N bond. The spectrogram of the LicA@CS-HA hydrogel demonstrated that the O-H and N-H stretching vibration absorption peak was located at 3283 cm^{-1} , the N-H bending vibration absorption peak was located at 1552 cm^{-1} , and the C-O bond stretching vibration absorption peak was located at 1153 cm^{-1} . At 1010 cm^{-1} was the stretching vibration absorption peak of the C-N bond. The results implied that the peak value of the LicA@CS-HA hydrogel was attenuated in different degrees due to LicA load. To evaluate the deformation behavior of the hydrogel during stretching, we further conducted tensile experiments on the hydrogel. As shown in Fig. 1E, the CS-HA hydrogel had a maximum strain at a break of 6% and a tensile strength of 2.6 Pa.

3.2 Physical properties of the LicA@CS-HA hydrogel

The rheological and mechanical properties of the CS-HA hydrogel and the LicA@CS-HA hydrogel were further evaluated. The results (Fig. 2A) of the CS-HA hydrogel variable strain scanning displayed that the G' gradually approached the G'' with the change of time in the process of strain increasing, and the condensed matter gradually approached the semi-solid state from the liquid state. On the other hand, with the change of time, the G' of the LicA@CS-HA hydrogel was gradually larger than G'' , which indicated the gel was still in the gel structure. Meanwhile, the gel state was in the morphology between solid and liquid, with certain viscosity and elasticity (Fig. 2B). The frequency scanning results of Fig. 2C and D expressed that G'' was greater than G' in the initial state of the CS-HA hydrogel and the LicA@CS-HA hydrogel, and G' intersected G'' as the frequency changes. When the amplitude frequency was greater than 45 Hz, G' was greater than G'' , then CS-HA hydrogel and the LicA@CS-HA hydrogel were in the gel state. We performed temperature scans to monitor the temperature stability of CS-HA hydrogel and LicA@CS-HA

hydrogel. Fig. 2 E implied that G' and G'' of CS-HA hydrogel were decreased with the increase of temperature. Near 45°C, G' intersected G'' , and then G' was greater than G'' , indicating that the sample was in a gel state during the treatment. As shown in Fig. 2F, the LicA@CS-HA hydrogel was in a sol state when G'' was greater than G' at 20°C to 45°C. When the temperature was close to 50°C, G' intersected G'' and the gel changed from sol state to gel state, indicating that the LicA@CS-HA hydrogel had certain thermal stability. The results of compression experiments showed (Fig. 2G, H) that the hydrogel would not break under 70% and 60% compression strain. The compressive stress values of the CS-HA hydrogel and the LicA@CS-HA hydrogel were 0.00006 Mpa and 0.00005 Mpa, respectively. When the pressure was removed, the hydrogel can return to its original form.

3.3 Biological properties of the LicA@CS-HA hydrogel

As illustrated in Fig. 3A, the LicA@CS-HA hydrogel had good adhesion to the heart, spleen, lungs, and skin of mice. Additionally, to evaluate the hemostatic properties of the LicA@CS-HA hydrogel, a rat tail-breaking experiment was performed. The results were proven in Fig. 3B, C. Tail hemorrhage was significantly reduced in rats treated with the LicA@CS-HA hydrogel compared to the control group. Then, the antimicrobial activity of the LicA@CS-HA hydrogel against *E. coli* and *S. aureus* was further evaluated. As can be seen in Fig. 3D, E, after 24 h intervention with the LicA@CS-HA hydrogel on *E. coli* and *S. aureus*, bacterial growth was significantly inhibited and the number of colonies was significantly reduced ($p < 0.01$). Compared with the control group, the inhibitory effects on *E. coli* and *S. aureus* were the LicA@CS-HA hydrogel group, the CS-HA hydrogel group, and the LicA group. Then the effect of hydrogel on the skin tissue of rat was observed by in vivo degradation experiment. As exhibited in Fig. 3F, the CS-HA hydrogel did not produce toxic effects on skin tissue. On day 7, inflammatory cells infiltrated the skin tissue. On the 14th day, the skin tissue structure was intact and a small amount of inflammatory cells could be seen.

3.4 LicA@CS-HA hydrogel promotes fibroblast proliferation and migration

The biocompatibility of the LicA@CS-HA hydrogel was assessed by CCK-8 cytotoxicity assay and cell migration assay. The results of the cytotoxicity assay demonstrated that the LicA group, the CS-HA hydrogel group, and the LicA@CS-HA hydrogel group could promote the proliferation of L929 cells compared with the control group (Fig. 4A), and the LicA@CS-HA

hydrogel group had the best proliferation effect. In addition, the results of the 24 h cell migration assay displayed that compared to the control group, the cell migration rate was significantly increased in the CS-HA hydrogel group and the LicA@CS-HA hydrogel group. Compared to the LicA group, the cell migration rate was increased in the LicA@CS-HA hydrogel group (Fig. 4B, C). The results of the CCK-8 cytotoxicity assay and cell migration assay were consistent, which proved that the LicA@CS-HA hydrogel had excellent security and the ability to promote the proliferation of L929 cells.

3.5 The LicA@CS-HA hydrogel promotes tissue regeneration and collagen fiber protein synthesis in wounds

As shown in Fig. 5A, B, the wound healing speed of the control group was slow, while the healing process of the LicA group, the CS-HA hydrogel group and the LicA@CS-HA hydrogel group was accelerated after treatment. Among them, the LicA@CS-HA hydrogel group had the fastest healing process ($p < 0.5$). The HE staining results on days 7 and 11 illuminated that the control group had incomplete wound healing, significant inflammation changes, and fewer new blood vessels. In contrast, the LicA, the CS-HA hydrogel and the LicA@CS-HA hydrogel groups had complete re-epithelialization, visible granulation tissue and new capillaries, and fewer inflammatory changes (Fig. 5C, D). Among them, the LicA@CS-HA hydrogel group had the best therapeutic effect. Additionally, the results in Fig. 5E displayed that compared with the control group, the collagen fiber expression in the CS-HA hydrogel group and the LicA@CS-HA hydrogel group was obviously increased ($p < 0.05$), of which the LicA@CS-HA hydrogel group had the most abundant collagen fiber expression on the 7th day ($p < 0.01$). On the 11th day (Fig. 5F), compared with the control group, the expression of collagen fibers in the LicA@CS-HA hydrogel group was significantly increased ($p < 0.05$), Masson staining changed from light blue to dark blue, and the collagen fibers were arranged orderly.

3.6 The LicA@CS-HA hydrogel promotes neovascularisation and accelerates wound healing

The expression of CD31, VEGF, and HIF-1 α in the wound tissues was observed by immunohistochemistry. As illuminated in Fig. 6A-D, compared with the control group, LicA group, the CS-HA hydrogel group and the LicA@CS-HA hydrogel group promoted the formation of wound neovascularization on day 7, in which the expressions of CD31, VEGF and HIF-1 α were significantly higher in the LicA@CS-HA hydrogel group ($p < 0.05$). In addition, compared with the

LicA, the CD31 and HIF-1 α positive expressions of the LicA@CS-HA hydrogel were obviously increased ($p < 0.05$). Compared with the CS-HA hydrogel group, CD31 expression of the LicA@CS-HA hydrogel was evidently increased ($p < 0.01$).

3.7 The LicA@CS-HA hydrogel modulates macrophage expression

To evaluate the effect of the LicA@CS-HA hydrogel on macrophages, we observed macrophage markers CD86 and CD206 expression by immunofluorescence staining on days 7 and 11 of wound healing. As illuminated in the result graphs on day 7 (Fig. 7A, B), the expression of CD86 was dramatically decreased in the LicA@CS-HA hydrogel group ($p < 0.01$) lower than those in the control group. Compared to the LicA group and the CS-HA group, the expression of CD86 in the LicA@CS-HA hydrogel group was markedly decreased ($p < 0.05$). As demonstrated in Fig. 7C, D, compared to the control group, CD206 expression was sensibly elevated in the LicA, the CS-HA, and the LicA@CS-HA hydrogel groups ($p < 0.05$). The expression of CD206 was significantly higher in the LicA@CS-HA hydrogel group compared to the LicA group and CS-HA group ($p < 0.01$). The immunofluorescence results on day 11 revealed (Fig. 7E, F) that CD86 expression was substantially reduced in the LicA@CS-HA hydrogel group compared with the control group ($p < 0.01$). Compared with the LicA group and the CS-HA hydrogel group, CD86 expression was also reduced in the LicA@CS-HA hydrogel group ($p < 0.05$). Meanwhile, CD206 expression (Fig. 7G, H) was obviously elevated in the LicA group, the CS-HA hydrogel group and the LicA@CS-HA hydrogel group by comparison to the control group ($p < 0.01$). In addition, the CD206 expression was markedly elevated in the LicA@CS-HA hydrogel group in compare to group of LicA ($p < 0.01$).

3.8 Molecular docking analysis

The binding between LicA and TNF- α /IL-6/IL-4/IL-10 proteins was verified based on molecular docking. In the docking results, Total_score ≥ 3 and Cscore ≥ 3 indicated that the active ingredient had a good binding with the target protein. Total_score > 7 indicated that had a strong binding activity. The scoring results of molecular docking were displayed in Tab 1. The LicA had good binding with with TNF- α /IL-6/IL-4/IL-10 proteins. The Total_scores between LicA and TNF- α /IL-6/IL-4/IL-10 proteins were all greater than 3, and the Cscores between LicA and TNF- α /IL-6/IL-4/IL-10 proteins were both over 3. According to the 3D results in Fig. 8A-D, LicA were all bound in the cavity pockets of the four proteins. The 2D results indicated the main types

of interaction between LicA and TNF- α protein include hydrogen bond and hydrophobic interaction. Hydrogen bonding stabilizes molecular docking complexes and improves binding specificity and affinity. Hydrophobic interactions help to bring the molecules together and reduce contact with water, thus reducing the system's energy and providing stability to the complex [31]. For example, the LicA formed a hydrogen bond with the residue TYR151. It formed a hydrophobic interaction with LEU57 and TYR59. The LicA formed hydrogen bonds with IL-6 protein residues ARG24 and LYS27 and formed alkyl interactions with TYR31 and ARG16. Alkyl interactions can help stabilize molecular docking complexes and increase binding affinity. Moreover, the contact area with water molecules can be reduced, lowering the system's free energy [32]. The LicA formed hydrogen bonds with IL-4 residues ALA35, THR39, and ARG115, and formed hydrophobic interactions with LYS37 and LYS123. The LicA formed hydrogen bonds with IL-10 protein residues LYS38 and GLN41, and formed alkyl interactions with PRO39, GLY40, and LYS43.

3.9 The LicA@CS-HA hydrogel modulates wound macrophage expression to inhibit inflammatory factor production

Subsequently, protein expression of inflammatory factors was analyzed by western blot on day 7 of wound healing (Fig. 9. A-G). Compared with the control group, the TNF- α expression was decreased in the LicA, the CS-HA, and the LicA@CS-HA hydrogel groups, and the effect of the LicA@CS-HA hydrogel group was more obvious. The expression of IL-6 in the CS-HA and the LicA@CS-HA hydrogel groups was evidently reduced in comparing with the control group ($p < 0.01$). Meanwhile, compared to the LicA group, the expressions of IL-6 and CD86 were significantly lower in the LicA@CS-HA hydrogel group ($p < 0.05$). In addition, we also observed the expression of anti-inflammatory factors. Compared to the control group, the expression level of the IL-4 was increased in the LicA@CS-HA hydrogel, the LicA and CS-HA groups. The expression level of IL-4 in the LicA@CS-HA group was significantly higher than that in the LicA and the CS-HA groups. The expression levels of IL-10 and CD206 in the LicA@CS-HA group were dramatically higher than those in the control group ($p < 0.05$). Compared to the control group, the expression level of CD206 in the CS-HA group was significantly higher ($p < 0.05$).

4. Discussion

The wound healing difficulty is related to the excessive inflammation caused by persistent

wound infection [33]. In order to promote wound healing, researchers are working on improving inflammatory responses and designing multifunctional wound dressings with antimicrobial properties [34]. At present, some antibacterial materials, such as CS, HA, sodium alginate, have been used in the preparation of wound dressings [35,36]. In view of the complexity of the wound environment, hydrogels have unique advantages. The inherent water content of hydrogels has a moisturizing effect on the wound, and the three-dimensional network structure can deliver drugs or cytokines [37]. The controlled release of active ingredients using hydrogel as carrier to promote wound healing is a new strategy for wound treatment in recent years [38].

With the deepening of the understanding and research of natural medicine, more and more attention has been paid to the application of traditional Chinese medicine and its monomer in clinic [39]. LicA is one of the flavonoids from licorice, which has many biological activities such as antioxidant, anti-inflammatory, antibacterial and anticancer [10,11]. The application of LicA is limited due to its poor water solubility and low bioavailability [12]. The combination of multifunctional hydrogels with natural medicines is a new way to enhance the effect of these natural medicines [13]. Hydrogel drug delivery technology is beneficial to the continuous release of active ingredients, reduce repeated administration, and improve the bioavailability of drugs [14]. Studies have illuminated that hydrogels can be classified into chemically cross-linked and physically cross-linked types. Chemical crosslinked hydrogels have limited their application and development in biomedicine due to their harmful reactions to biological activity. In contrast, physically cross-linked hydrogels are formed through ionic interactions, protein interactions and hydrogen bonding. No crosslinkers are involved in the preparation process, so it is safe [40]. Polysaccharides are one of the common matrix components of physically crosslinked hydrogels, which can provide a physical barrier to protect the loaded substance from the external environment. CS is a natural alkaline polysaccharide derived from the deacetylation of chitin, which has the advantages of nontoxicity, antimicrobial, antioxidant, and biocompatibility, and has the potential to deliver active substances [41]. HA belongs to the glycosaminoglycan family and is one of the most important components of the extracellular matrix. HA has unique physicochemical properties such as hydrophilicity, fluidity, viscoelasticity and antioxidant properties [42]. The positive charges on CS and the negative charges on HA attract each other, and this electrostatic attraction causes the molecular chains to become entangled with each other and

form the CS-HA hydrogels. Lin et al. also reported that the CS-HA hydrogel has better biocompatibility and safety [43]. Studies have shown that the CS-HA hydrogel can provide a moist environment for wound surface, promote air exchange and angiogenesis [43]. As a barrier for microorganisms, it can remove excessive exudate and accelerate wound healing [15,16]. In this experiment, the LicA was selected as a drug carrier to be loaded into the CS-HA hydrogel to explore its effect on wound healing.

In this study, the CS-HA hydrogel and the LicA@CS-HA hydrogel were prepared by physical crosslinking method. The SEM showed that LicA@CS-HA hydrogel has a three-dimensional network structure and can be used as a good carrier for drug delivery. The results of drug release illuminated that the LicA loaded in CS-HA hydrogel reached the peak release on the 5th day, and the CS-HA hydrogel effectively improved the utilization rate of the LicA. It may be attributed to the three-dimensional mesh structure and smaller pore structure of the CS-HA hydrogel, where drug molecules can be encapsulated in the gel, thus prolonging drug release [44]. In addition, there is hydrogen bonding between the hydrogel and the drug molecules, and the formation of hydrogen bonding can enhance the binding force between the drug and the hydrogel, thus slowing down the drug release rate [45]. The payload of LicA was further verified by FTIR detection, and it was found that the peak value of the LicA@CS-HA hydrogel spectral diagram was weakened, which may be due to the influence of LicA. The results of the tensile experiments showed that the CS-HA hydrogels possessed tensile properties, which could be attributed to the flexibility due to the amino and hydroxyl functional groups of CS and the good elasticity due to the three-dimensional mesh structure of HA [46]. The rheological experiments and mechanical properties demonstrated that the LicA@CS-HA hydrogel had good elastic deformation ability, thermal stability and good compressive stress. In addition, the hemostatic experiment showed that the LicA@CS-HA hydrogel had good hemostatic performance compared with the control group. It is related to the positive charge carried by CS and the negative charge on the surface of red blood cells to promote red blood cell adhesion, aggregation, and coagulation [47]. The LicA@CS-HA hydrogel adhesion results indicated that it can be firmly covered on the wound surface, providing a good physical barrier for the wound surface. The LicA@CS-HA hydrogel had good adhesion, which could absorb blood and moisture from the wound surface, and make coagulation factors aggregate to produce the hemostatic effect.

Studies have shown that exposure to air can easily lead to bacterial infection and delay healing, so hydrogels with strong antibacterial properties have more clinical application value [48]. The antibacterial activity of the LicA@CS-HA hydrogel on *S. aureus* and *E. coli* was evaluated. The results showed that the LicA@CS-HA hydrogel had excellent antibacterial activity, and its inhibitory effects on *S. aureus* and *E. coli* were as high as 93% and 99%, which may be related to the LicA and CS contained in the LicA@CS-HA hydrogel. Studies have shown that the LicA has inhibitory effects on a variety of pathogenic bacteria, such as *S. aureus*, *E. coli*, *bifidobacterium* and *pusillanimous bacillus* [49]. In addition, the molecular weight and positive charge density of CS are also key factors affecting its antibacterial activity [50]. The positive charge of CS can interact with bacterial cell membranes, change the permeability of bacterial cell walls, and finally promote bacterial death [51].

Biocompatibility is one of the most important parameters to evaluate the potential application of hydrogels in tissue engineering, and it is also the basic premise for the application of biomaterials in wound repair [52]. In this study, the results of cytotoxicity and migration showed that compared with the control group, the LicA@CS-HA hydrogel did not reduce the number of L929 fibroblasts, and promoted the proliferation and migration of L929 fibroblasts. This can be interpreted as the interaction that CS can provide cell morphology and communication between cells, as well as cell adhesion, thus promoting cell proliferation and differentiation [53]. Meanwhile, HA has a good interaction with cell matrix and cell surface receptor proteins, and can also promote cell migration and proliferation [54]. Our research displayed that the LicA@CS-HA Hydrogel had good cellular biocompatibility.

A series of experimental results exhibited that the LicA@CS-HA hydrogel had ideal properties as wound dressing. The effect of LicA@CS-HA hydrogel dressing on promoting wound healing was studied in mice wound model. At the 0, 3, 5, 7, 9 and 11 days after surgery, the wound size changes of different treatment groups showed that the wound area of the LicA@CS-HA hydrogel group was sensibly smaller than that of the control group. Moreover, 9 days after injury, obvious scab could be observed at the wound site in the control group, while no similar result was observed in the LicA@CS-HA hydrogel group. This was due to the fact that the LicA@CS-HA hydrogel had good permeability and the ability to absorb wound exudates, which can keep the wound area dry. These results were consistent with previous reports that the CS-HA hydrogels

could maintain gas exchange at the wound site and absorb excess wound exudates [55]. The results of H&E staining and Masson staining also showed that compared with the control group, the number of angiogenesis and collagen deposition at the skin wound site of mice were significantly increased after treatment with the LicA@CS-HA hydrogel, and the wound healing was more complete. In addition, we also found that the CS-HA hydrogel can also promote wound healing. This can be attributed to the fact that the CS-HA hydrogel can provide a moist healing environment for wounds, which is conducive to cell proliferation and migration [56]. Secondly, the CS-HA hydrogel has good antibacterial properties. It can reduce the risk of wound infection and create a good healing environment. In addition, the CS-HA hydrogel also has good biocompatibility and the ability to promote angiogenesis. The new blood vessels can provide sufficient oxygen and nutrients to the wound and promote wound healing.

Abnormal inflammatory response is an important factor in wound healing. Macrophages, as the core cells of inflammatory response, can clear infection sources and damaged tissue cells and promote tissue repair and regeneration. The failure of proinflammatory macrophages (M1) to transform into anti-inflammatory macrophages (M2) in time is the main reason for unresolved wound inflammation [57]. Persistent inflammation prevents the wound from transitioning to the proliferative stage, which leads to impaired wound healing. Normally, M1 macrophages promote an early transient inflammatory response by secreting a variety of high levels of pro-inflammatory factors, such as IL-6, IL-1 β and TNF- α , to clear necrotic tissue debris and pathogens around the wound [57]. Subsequently, macrophages are polarized into M2 state and secrete a variety of growth factors and anti-inflammatory cytokines, such as IL-10, IL-4 and CD206, which regulate the proliferation and differentiation of cells around the wound during the advanced inflammatory reaction, thus ensuring the timely and effective healing of normal wounds [58]. On the contrary, M1-type macrophages in the wound cannot be timely polarized into M2-type giant cells, which will lead to a long-term and persistent inflammatory state, inhibit angiogenesis and collagen deposition, and eventually lead to delayed wound healing or non-healing [57, 59]. Therefore, it is an effective method to promote the polarization of macrophages to M2 phenotype in time.

Based on the polarization of macrophages, this study explored the role of the LicA@CS-HA hydrogel in promoting wound healing in mice. After 7 and 14 days of trauma, immunofluorescence showed that CD86 expression was decreased in all groups, CD206

expression was increased in all groups, and the inflammatory response was subsided. The LicA@CS-HA hydrogel had stronger anti-inflammatory effect than the CS-HA hydrogel and the LicA group, indicating that the LicA@CS-HA hydrogel could accelerate tissue healing by reducing the inflammatory response. Western blot analysis also showed that the LicA@CS-HA hydrogel group could better inhibit the production of inflammatory factors TNF- α , IL-6 and CD86, and promote the expression of anti-inflammatory factors IL-4, IL-10 and CD206. It was fully verified that the LicA@CS-HA hydrogel has the ability to regulate giant cell polarization and make giant cells polarize from M1 type to M2 type. Molecular docking results also verified the interaction of the LicA with pro-inflammatory and anti-inflammatory factors in macrophages. It has been reported that the LicA can inhibit the expression of pro-inflammatory mediators, such as TNF- α , IL-6 and IL-1 β , thereby improving the production of inflammatory response [15,16], suggesting that it was related to the acceleration of the wound healing process. Liu et al. reported that LicA has a powerful anti-inflammatory effect and can regulate the release of IL-4, IL-10 and other cytokines [60]. Chu et al. proved that LicA could significantly inhibit the production of TNF- α and IL-6 induced by lipopolysaccharide (LPS) [61]. This is consistent with our findings that LicA improves inflammatory responses during wound tissue healing. Moreover, HA as the main component of extracellular matrix, can regulate and promote the occurrence of cell proliferation, cell adhesion and cell migration, thus promoting the process of wound healing [27,28].

In addition, the expressions of CD31 and VEGF were increased in immunohistochemical staining, which further indicated that the LicA@CS-HA hydrogel could accelerate wound healing by promoting the formation of new blood vessels, which was also verified by the results of HE staining. This is consistent with the results reported in the literature [10] that M2 macrophages can induce angiogenesis by producing VEGF, which is conducive to wound repair. As reported in the literature, neovascularization is also necessary for wound healing and can help build granulation tissue and promote tissue regeneration [11]. On the other hand, the increase of HIF-1 α in the LicA@CS-HA hydrogel group also suggested that CS-HA hydrogel loaded LicA could promote the construction of ECM by accelerating the deposition of collagen, and the results were consistent with Masson staining. Our study displayed that the LicA@CS-HA hydrogel may be a

potential therapeutic modality to accelerate wound repair.

5. Conclusion

The LicA@CS-HA hydrogel was prepared successfully. The hydrogel had good elastic deformation ability, thermal stability, good compressive stress, three-dimensional space network structure, adhesion and hemostatic performance. It had the potential to better absorb wound exudate and biocompatibility when applied as a wound dressing, providing conditions for the storage and sustained release of drug molecules. The prepared LicA@CS-HA hydrogel had good antibacterial performance against common pathogenic bacteria *S. aureus* and *E. coli* in wound infection. In wound experiments in mice, the LicA@CS-HA hydrogel can enhance wound contraction, promote angiogenesis, cell proliferation and collagen deposition at the wound site, induce macrophages to polarization towards M2 phenotype, reduce inflammation, thus accelerate wound healing in mice, which has potential application prospects in wound healing.

Declaration of Competing Interest

The authors declare no conflicts of interest.

Fund

The research was supported by the Shenyang Science and Technology Plan Project (22-315-6-17) and the Shenyang Natural Science Foundation Special Project (23-503-6-14).

Reference

- [1] M. Li, Q. Hou, L. Zhong, Y. Zhao, X. Fu, Macrophage Related Chronic Inflammation in Non-Healing Wounds, *Front Immunol.* 12 (2021) 681710.
- [2] Z.J. Liu, O.C. Velazquez, Hyperoxia, endothelial progenitor cell mobilization, and diabetic wound healing, *Antioxid Redox Signal.* 10(11) (2008) 1869-1882.
- [3] S.J. Wolf, W.J. Melvin, K. Gallagher, Macrophage-mediated inflammation in diabetic wound repair, *Semin Cell Dev Biol.* 119 (2021) 111-118.
- [4] P. Krzyszczyk, R. Schloss, A. Palmer, F. Berthiaume, The Role of Macrophages in Acute and Chronic Wound Healing and Interventions to Promote Pro-wound Healing Phenotypes, *Front Physiol.* 9 (2018) 419.
- [5] Q. Li, Y. Niu, P. Xing, C. Wang, Bioactive polysaccharides from natural resources including Chinese medicinal herbs on tissue repair, *Chin Med.* 13 (2018) 7.
- [6] F.L. Li, G.C. Wang, B.Q. Wu, Clinical application of traditional Chinese medicine powder in the treatment of acute and chronic wounds, *Int Wound J.* 20 (3) (2023) 799-805.
- [7] B. Yan, J. Hou, W. Li, L. Luo, M. Ye, Z. Zhao, W. Wang, A review on the plant resources of important medicinal licorice, *J Ethnopharmacol.* 301 (2023) 115823.
- [8] X. Tao, Y. Hu, N. Mao, M. Shen, M. Fang, M. Zhang, J. Lou, Y. Fang, X. Guo, Z. Lin, Echinatin alleviates inflammation and pyroptosis in hypoxic-ischemic brain damage by inhibiting TLR4/ NF- κ B pathway, *Int Immunopharmacol.* 136 (2024) 112372.

- [9] R.J. Nijveldt, E. van Nood, D.E. van Hoorn, P.G. Boelens, K. van Norren, P.A. van Leeuwen, Flavonoids: a review of probable mechanisms of action and potential applications, *Am J Clin Nutr.* 74 (4) (2001) 418-425.
- [10] Y. Ding, E. Brand, W. Wang, Z. Zhao, Licorice: Resources, applications in ancient and modern times, *J Ethnopharmacol.* 298 (2022) 115594.
- [11] R. Sharma, R.K. Singla, S. Banerjee, R. Sharma, Revisiting Licorice as a functional food in the management of neurological disorders: Bench to trend, *Neurosci Biobehav Rev.* 155 (2023) 105452.
- [12] R. Shi, Y. Liu, Y. Ma, P. Zhao, Z. Jiang, J. Hou, pH-Dependent Binding Behavior of the α -Lactalbumin/Glycyrrhizic Acid Complex in Relation to Their Foaming Characteristics in Bulk, *J Agric Food Chem.* 70 (10) (2022) 3252-3262.
- [13] Y. Liu, Z. Hong, J. Qian, Y. Wang, S. Wang, Protective effect of Jie-Geng-Tang against *Staphylococcus aureus* induced acute lung injury in mice and discovery of its effective constituents, *J Ethnopharmacol.* 243 (2019) 112076.
- [14] L. Wang, R. Yang, B. Yuan, Y. Liu, C. Liu, The antiviral and antimicrobial activities of licorice, a widely-used Chinese herb, *Acta Pharm Sin B.* 5(4) (2015) 310-315.
- [15] M.N. Asl, H. Hosseinzadeh, Review of pharmacological effects of *Glycyrrhiza* sp. and its bioactive compounds, *Phytother Res.* 22 (6) (2008) 709-724.
- [16] H.T.L. Phan, H.J. Kim, S. Jo, W.K. Kim, W. Namkung, J.H. Nam, Anti-Inflammatory Effect of Licochalcone A via Regulation of ORA11 and K⁺ Channels in T-Lymphocytes, *Int J Mol Sci.* 22 (19) (2021) 10847.
- [17] H. Cao, L. Duan, Y. Zhang, J. Cao, K. Zhang, Current hydrogel advances in physicochemical and biological response-driven biomedical application diversity, *Signal Transduct Target Ther.* 6 (1) (2021) 426.
- [18] C. Huang, L. Dong, B. Zhao, Y. Lu, S. Huang, Z. Yuan, G. Luo, Y. Xu, W. Qian, Anti-inflammatory hydrogel dressings and skin wound healing, *Clin Transl Med.* 12 (11) (2022) e1094.
- [19] L.E. Kass, J. Nguyen, Nanocarrier-hydrogel composite delivery systems for precision drug release, *Wiley Interdiscip Rev Nanomed Nanobiotechnol.* 14 (2) (2022) e1756.
- [20] B. Vigani, S. Rossi, G. Sandri, M.C. Bonferoni, C.M. Caramella, F. Ferrari, Hyaluronic acid and chitosan-based nanosystems: a new dressing generation for wound care, *Expert Opin Drug Deliv.* 16 (7) (2019) 715-740.
- [21] C.J. Park, S.G. Clark, C.A. Lichtensteiger, R.D. Jamison, A.J. Johnson, Accelerated wound closure of pressure ulcers in aged mice by chitosan scaffolds with and without bFGF, *Acta Biomater.* 5 (6) (2009) 1926-1936.
- [22] P. Simard, H. Galarneau, S. Marois, D. Rusu, C.D. Hoemann, P.E. Poubelle, H. El-Gabalawy, M.J. Fernandes, Neutrophils exhibit distinct phenotypes toward chitosans with different degrees of deacetylation: implications for cartilage repair, *Arthritis Res Ther.* 11 (3) (2009) R74.
- [23] A. Alnazza Alhamad, S. Zeghoud, I. Ben Amor, H. Hemmami, Chitosan-based hydrogels for wound healing: correspondence, *Int J Surg.* 109 (6) (2023) 1821-1822.
- [24] M.F.P. Graça, S.P. Miguel, C.S.D. Cabral, I. J. Correia, Hyaluronic acid-Based wound dressings: A review, *Carbohydr Polym.* 241 (2020) 116364.
- [25] M. Gruppuso, F. Iorio, G. Turco, E. Marsich, D. Porrelli, Hyaluronic acid/lactose-modified chitosan electrospun wound dressings - Crosslinking and stability criticalities, *Carbohydr Polym.* 288 (2022) 119375.
- [26] H. Ren, Z. Zhang, X. Cheng, Z. Zou, X. Chen, C. He, Injectable, self-healing hydrogel adhesives with firm tissue adhesion and on-demand biodegradation for sutureless wound closure, *Sci Adv.* 9(33) (2023) eadh4327.
- [27] A.P. Veith, K. Henderson, A. Spencer, A.D. Sligar, A.B. Baker, Therapeutic strategies for enhancing angiogenesis in wound healing, *Adv Drug Deliv Rev.* 146 (2019) 97-125.
- [28] Z. Luo, J. Xu, Q. Gao, Z. Wang, M. Hou, Y. Liu, Study on the effect of licochalcone A on intestinal flora in

- type 2 diabetes mellitus mice based on 16S rRNA technology, *Food Func.* 14 (19) (2023) 8903-8921.
- [29] F. Hou, Z. Yu, Y. Cheng, Y. Liu, S. Liang, F. Zhang, Deciphering the pharmacological mechanisms of *Scutellaria baicalensis* Georgi on oral leukoplakia by combining network pharmacology, molecular docking and experimental evaluations, *Phytomedicine*. 103 (2022) 154195.
- [30] N.T. Nguyen, T.H. Nguyen, T.N.H. Pham, N.T. Huy, M.V. Bay, M.Q. Pham, P.C. Nam, V.V. Vu, S.T. Ngo, Autodock Vina Adopts More Accurate Binding Poses but Autodock4 Forms Better Binding Affinity, *J Chem Inf Model*. 60 (1) (2020) 204-211.
- [31] S. C. DK. S, V. Ragunathan, P. Tiwari, S. A, BD. P, Molecular docking, validation, dynamics simulations, and pharmacokinetic prediction of natural compounds against the SARS-CoV-2 main-protease. *J Biomol Struct Dyn*. 40,2 (2022): 585-611.
- [32] H. Rai, A. Barik, Y.P. Singh, et al., Molecular docking, binding mode analysis, molecular dynamics, and prediction of ADMET/toxicity properties of selective potential antiviral agents against SARS-CoV-2 main protease: an effort toward drug repurposing to combat COVID-19. *Mol Divers*. 25,3 (2021): 1905-1927.
- [33] A. Schmidt, T. von Woedtke, B. Vollmar, S. Hasse, S. Bekeschus, Nrf2 signaling and inflammation are key events in physical plasma-spurred wound healing, *Theranostics*. 9 (4) (2019) 1066-1084.
- [34] W. Liu, R. Gao, C. Yang, Z. Feng, W. Ou-Yang, X. Pan, P. Huang, C. Zhang, D. Kong, W. Wang, ECM-mimetic immunomodulatory hydrogel for methicillin-resistant *Staphylococcus aureus*-infected chronic skin wound healing, *Sci Adv*. 8 (27) (2022) eabn7006.
- [35] M. Hao, C. Ding, S. Sun, X. Peng, W. Liu, Chitosan/Sodium Alginate/Velvet Antler Blood Peptides Hydrogel Promotes Diabetic Wound Healing via Regulating Angiogenesis, Inflammatory Response and Skin Flora, *J Inflamm Res*. 15 (2022) 4921-4938.
- [36] Y. Wang, Y. Zhang, Y.P. Yang, et al., Versatile dopamine-functionalized hyaluronic acid-recombinant human collagen hydrogel promoting diabetic wound healing via inflammation control and vascularization tissue regeneration, *Bioact Mater*. 35 (2024) 330-345.
- [37] Y.J. Fu, Y.F. Shi, L.Y. Wang, et al., All-Natural Immunomodulatory Bioadhesive Hydrogel Promotes Angiogenesis and Diabetic Wound Healing by Regulating Macrophage Heterogeneity, *Adv Sci*. (2024) e2404890.
- [38] Z. Li, J. Liu, J. Song, et al., Multifunctional hydrogel-based engineered extracellular vesicles delivery for complicated wound healing, *Theranostics*. 14 (11) (2024) 4198-4217.
- [39] A.G. Atanasov, S.B. Zotchev, V.M. Dirsch, International Natural Product Sciences Taskforce, Supuran CT. Natural products in drug discovery: advances and opportunities, *Nat Rev Drug Discov*. 20 (3) (2021) 200-216.
- [40] X. Hu, L. Zhang, L. Yan, L. Tang, Recent Advances in Polysaccharide-Based Physical Hydrogels and Their Potential Applications for Biomedical and Wastewater Treatment. *Macromol Biosci*. 9 (2022) e2200153.
- [41] X. Wei, C. Liu, Z. Li, Z. Gu, J. Yan, K. Luo, Chitosan-based hydrogel dressings for diabetic wound healing via promoting M2 macrophage-polarization. *Carbohydr Polym*. 331 (2024) 121873.
- [42] J. Zhou, Y. Liu, X. Li, et al., Hyaluronic acid-based dual network hydrogel with sustained release of platelet-rich plasma as a diabetic wound dressing. *Carbohydr Polym*. 314 (2023) 120924.
- [43] Y. Lin, J. Xu, Y. Dong, et al., Drug-free and non-crosslinked chitosan/hyaluronic acid hybrid hydrogel for synergistic healing of infected diabetic wounds. *Carbohydr Polym*. 314 (2023) 120962.
- [44] TS. Anirudhan, M. Mohan, MR. Rajeev, Modified chitosan-hyaluronic acid based hydrogel for the pH-responsive Co-delivery of cisplatin and doxorubicin. *Int J Biol Macromol*. 201 (2022) 378-388.
- [45] Y. Cai, L. Xin, H. Li, P. Sun, C. Liu, L. Fang, Mussel-inspired controllable drug release hydrogel for transdermal drug delivery: Hydrogen bond and ion-dipole interactions. *J Control Release*. 365 (2024)

- 161-175.
- [46] S. Maiz-Fernández, L. Pérez-Álvarez, U. Silván, JL. Vilas-Vilela, S. Lanceros-Mendez, Photocrosslinkable and self-healable hydrogels of chitosan and hyaluronic acid. *Int J Biol Macromol.* 216 (2022) 291-302.
- [47] F. Song, Y. Kong, C. Shao, et al. Chitosan-based multifunctional flexible hemostatic bio-hydrogel. *Acta Biomater.* 136 (2021): 170-183.
- [48] L. Qiao, Y. Liang, J. Chen, et al., Antibacterial conductive self-healing hydrogel wound dressing with dual dynamic bonds promotes infected wound healing, *Bioact Mater.* 30 (2023) 129-141.
- [49] F. Shen, Y. Zhang, C. Li, H. Yang, P. Yuan, Network pharmacology and experimental verification of the mechanism of licochalcone A against *Staphylococcus aureus* pneumonia, *Front Microbiol.* 15 (2024) 1369662.
- [50] H. Tang, P. Zhang, T.L. Kieft, et al., Antibacterial action of a novel functionalized chitosan-arginine against Gram-negative bacteria, *Acta Biomater.* 6 (7) (2010) 2562-2571.
- [51] D.P. Rahayu, A. De Mori, R. Yusuf, R. Draheim, A. Lalatsa, M. Roldo, Enhancing the antibacterial effect of chitosan to combat orthopaedic implant-associated infections, *Carbohydr Polym.* 289 (2022) 119385.
- [52] Z. Yang, R. Huang, B. Zheng, et al., Highly Stretchable, Adhesive, Biocompatible, and Antibacterial Hydrogel Dressings for Wound Healing, *Adv Sci.* 8(8) (2021) 2003627.
- [53] C. Zhou, T. Jiang, S. Liu, Y. He, G. Yang, J. Nie, F. Wang, X. Yang, Z. Chen, C. Lu, AgNPs loaded adenine-modified chitosan composite POSS-PEG hybrid hydrogel with enhanced antibacterial and cell proliferation properties for promotion of infected wound healing, *Int J Biol Macromol.* 267 (Pt 1) (2024)131575.
- [54] K. Chen, Y. Liu, X. Liu, et al., Hyaluronic acid-modified and verteporfin-loaded polylactic acid nanogels promote scarless wound healing by accelerating wound re-epithelialization and controlling scar formation, *J Nanobiotechnology.* 21 (1) (2023) 241.
- [55] N. Yuan, K. Shao, S. Huang, C. Chen, Chitosan, alginate, hyaluronic acid and other novel multifunctional hydrogel dressings for wound healing: A review, *Int J Biol Macromol.* 240 (2023) 124321.
- [56] J. Alkabli. Recent advances in the development of chitosan/hyaluronic acid-based hybrid materials for skin protection, regeneration, and healing: A review. *Int J Biol Macromol.* 3 (2024) 135357.
- [57] C.O. Audu, W.J. Melvin, A.D. Joshi, et al., Macrophage-specific inhibition of the histone demethylase JMJD3 decreases STING and pathologic inflammation in diabetic wound repair, *Cell Mol Immunol.* 19 (11) (2022) 1251-1262.
- [58] Z. Zhou, T. Deng, M. Tao, et al., Snail-inspired AFG/GelMA hydrogel accelerates diabetic wound healing via inflammatory cytokines suppression and macrophage polarization, *Biomaterials.* 299 (2023) 122141.
- [59] S. Li, X. Ding, H. Zhang, Y. Ding, Q. Tan, IL-25 improves diabetic wound healing through stimulating M2 macrophage polarization and fibroblast activation, *Int Immunopharmacol.* 106 (2022) 108605.
- [60] M. Liu, Y. Du, D. Gao, Licochalcone A, a review of its pharmacology activities and molecular mechanisms. *Front Pharmacol.* 15 (2024) 1453426.
- [61] X. Chu, X. Ci, M. Wei, et al., Licochalcone A inhibits lipopolysaccharide-induced inflammatory response in vitro and in vivo. *J Agric Food Chem.* 15 (2012) 3947-54.

Fig. 1. Structural characterization of the LicA@CS-HA hydrogel. (A) Preparation of the LicA@CS-HA hydrogel. (B) Scanning electron microscopy (SEM) structures of the LicA, CS-HA hydrogel and LicA@CS-HA hydrogel, Red arrows: LicA. (C) In vitro release analysis and quantification of LicA from the LicA@CS-HA hydrogel. (D) The FTIR characterization of the LicA@CS-HA hydrogel. (E) Tensile property results of the CS-HA hydrogel.

Fig. 2. Analysis of rheological and mechanical properties of the CS-HA hydrogel and LicA@CS-HA hydrogel. (A, B) Variable strain scanning results of CS-HA hydrogel (left) and LicA@CS-HA hydrogel (right). (C, D) The frequency scan results of CS-HA hydrogel (left) and LicA@CS-HA hydrogel (right). (E, F) The temperature scan results of CS-HA hydrogel (left) and LicA@CS-HA hydrogel (right). (G, H) The evaluation of mechanical properties of the CS-HA hydrogel and the LicA@CS-HA hydrogel.

Fig. 3. Evaluation of physical properties of the LicA@CS-HA hydrogel. (A) Evaluation of adhesion properties of the LicA@CS-HA hydrogel. (B) Short-tail hemostasis test in the rats. (C) Statistics of 3 min (left) and 5 min (right) hemorrhage in each experimental group. (D) Antibacterial activity of the LicA@CS-HA hydrogel against *E. coli* and *S. aureus*. (E) Statistical graph of antibacterial activity of each experimental group. The data were presented as mean \pm SD (n=3). ** p <0.01 as compared to the control group, ### p <0.01 as compared to the LicA group and the CS-HA hydrogel. (F) Degradation of the CS-HA hydrogel in rat skin tissue. Blue arrows: the CS-HA hydrogel implant site, scale bars were 100 μ m.

Fig. 4. The biocompatibility of LicA@CS-HA hydrogel. (A) Statistical graph of CCK-8 cytotoxicity assay. (B) Quantification of cell migration experiments. (C) The results of 24 h L929 cells migration assay, scale bars are 40 \times . The data were presented as mean \pm SD (n=3). ** p <0.01 as compared to the control group, ### p <0.01 as compared to the LicA group and the CS-HA hydrogel.

Fig. 5. The LicA@CS-HA hydrogel promotes wound tissue regeneration and collagen fiber protein synthesis. (A, B) Wound healing in mice from 0-11 days and statistical analysis. (C-F) The plot and statistical analysis of the results of HE staining and Masson staining of traumatized

tissues on day 7 and day 11. The data were presented as mean \pm SD. * p <0.05 and ** p <0.01 as compared to the control group, scale bars of HE were 200 μ m.

Fig. 6. Immunohistochemistry results were plotted on days 7 and 11. (A-D) The pro-angiogenic capacity of each experimental group was assessed on day 7. Red arrows: neovascularisation, black arrows: fibroblasts, scale bars were 20 μ m in the immunohistochemistry. The data were presented as mean \pm SD. * p <0.05 and ** p <0.01 compared to the control group, # p <0.05 and ## p <0.01 compared to the LicA group and the CS-HA hydrogel.

Fig. 7. The LicA@CS-HA hydrogel regulates macrophage expression. (A-D) Quantification of CD86 and CD206 positive cells in the wound area of the control, the LicA, the CS-HA hydrogel, and the LicA@CS-HA hydrogel groups on day 7 of wound healing. (E-H) The expression of CD86 and CD206 positive cells in the wound area of each experimental group on day 11 of wound healing. Scale bars were 200 μ m. The data were presented as mean \pm SD. ** p <0.01 compared to the control group, # p <0.05 and ## p <0.01 compared to the LicA group and the CS-HA hydrogel.

Fig. 8. Molecular docking studies of LicA binding to TNF- α /IL-6/IL-4/IL-10 proteins.

Fig. 9. Analysis of protein expression of M1 and M2 markers and inflammatory factors. (A-G) The expression of relevant proteins on day 7 and quantitative analyses. The data were presented as mean \pm SD. * p <0.05 and ** p <0.01 as compared to the control group, # p <0.05 and ## p <0.01 as compared to the LicA group and the CS-HA hydrogel.

Table 1. Docking score of LicA with TNF- α /IL-6/IL-4/IL-10 proteins.

Protein	Total-Score	CSCOR
TNF- α	7.2098	4
IL-6	4.2302	5
IL-4	4.9932	5
IL-10	3.7203	3

Declaration of interests

The authors declare that they have no known competing financial interests or personal relationships that could have appeared to influence the work reported in this paper.

Highlights

- This research developed a new hydrogel delivery system (LicA@CS-HA Hydrogel).
- LicA@CS-HA hydrogel delivery system had good biocompatibility and antibacterial activity.
- LicA@CS-HA hydrogel in promoting wound healing may be related to the regulation of macrophage polarisation.
- Molecular docking confirmed that LicA interacted with TNF- α /IL-6/IL-4/IL-10 proteins.

Journal Pre-proof

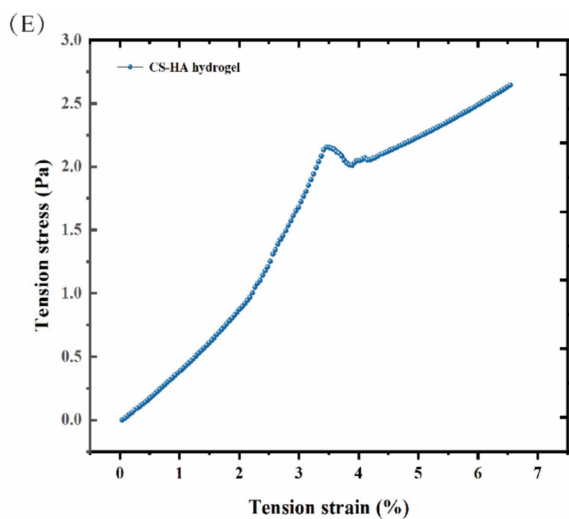
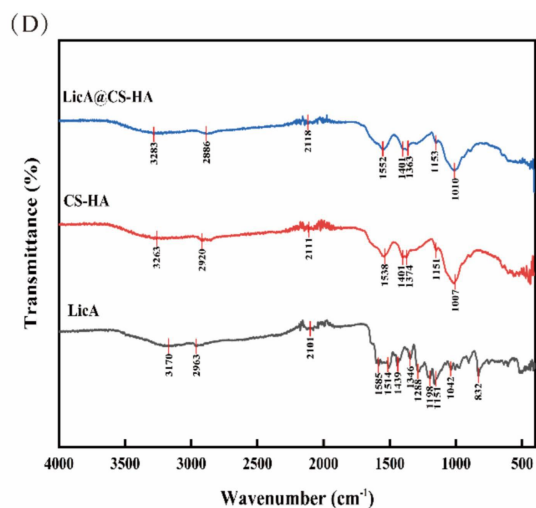
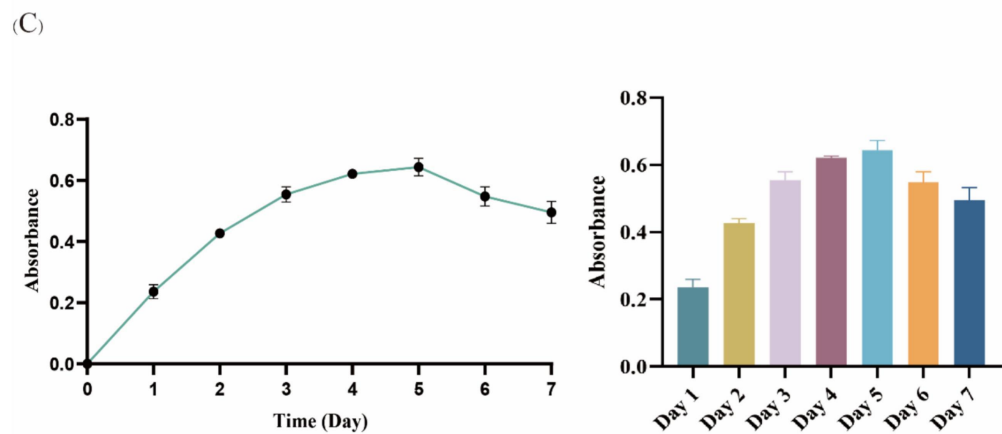
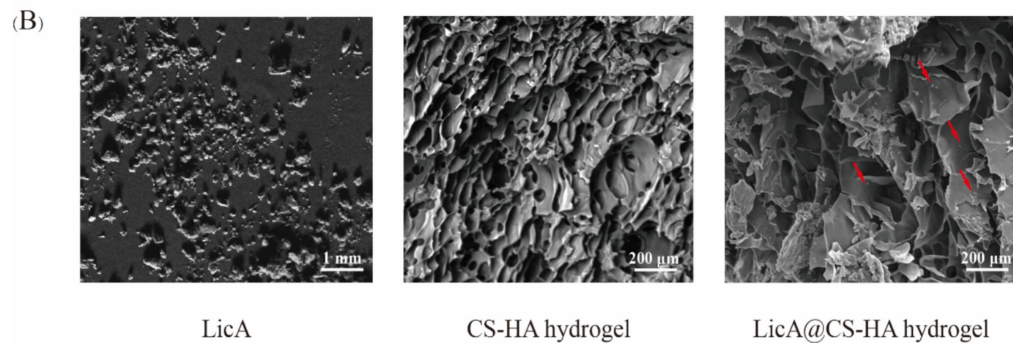
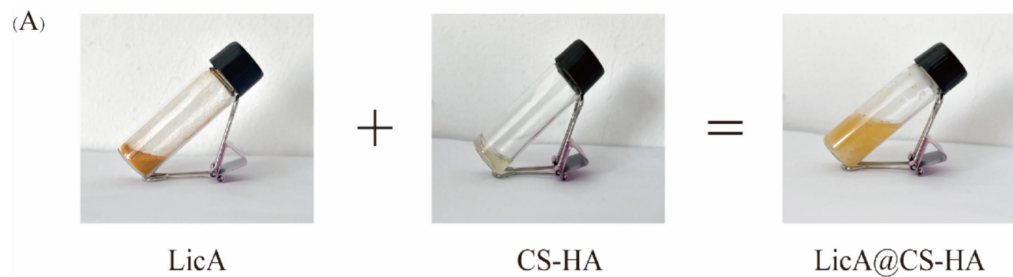


Figure 1

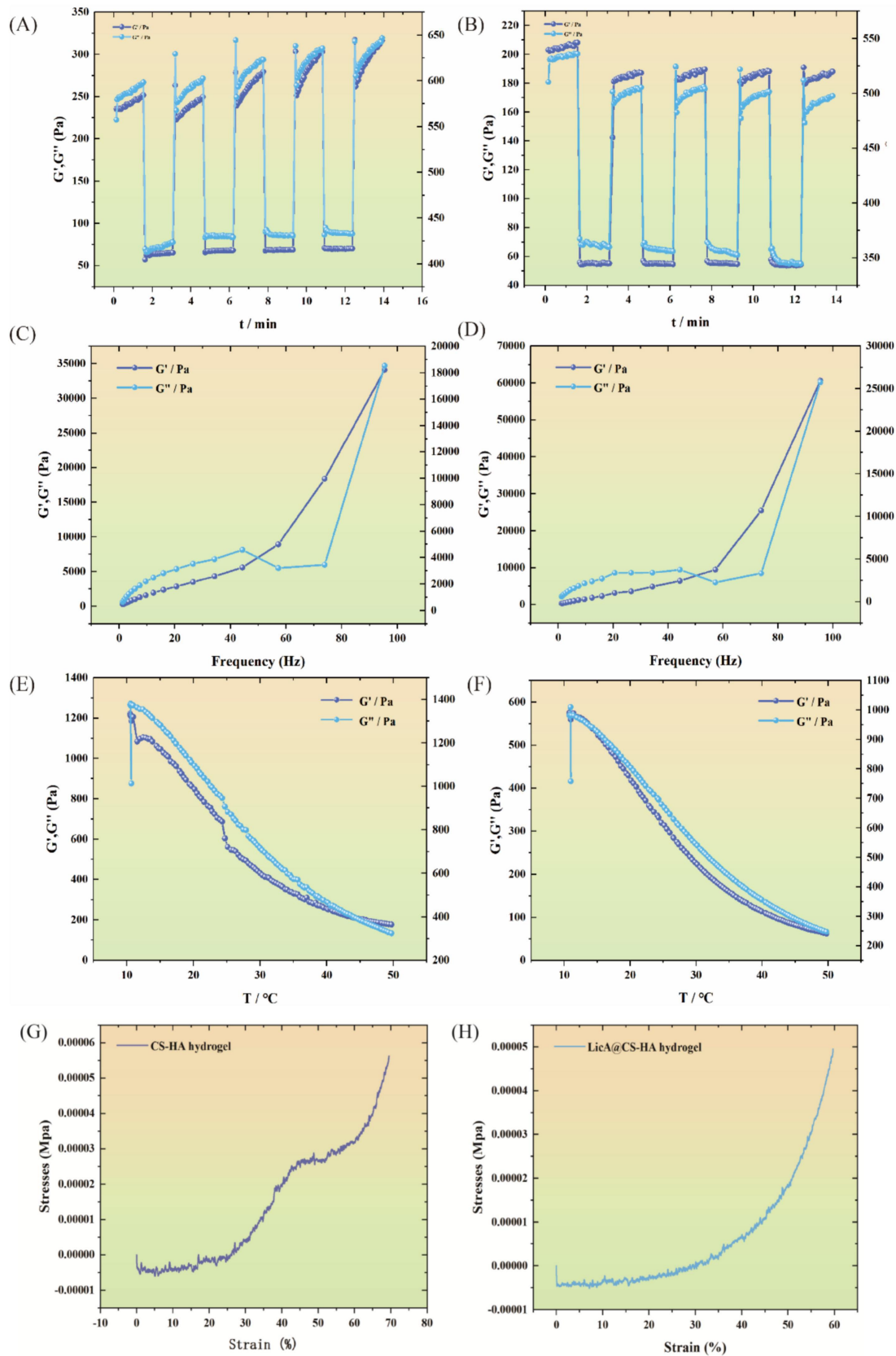


Figure 2

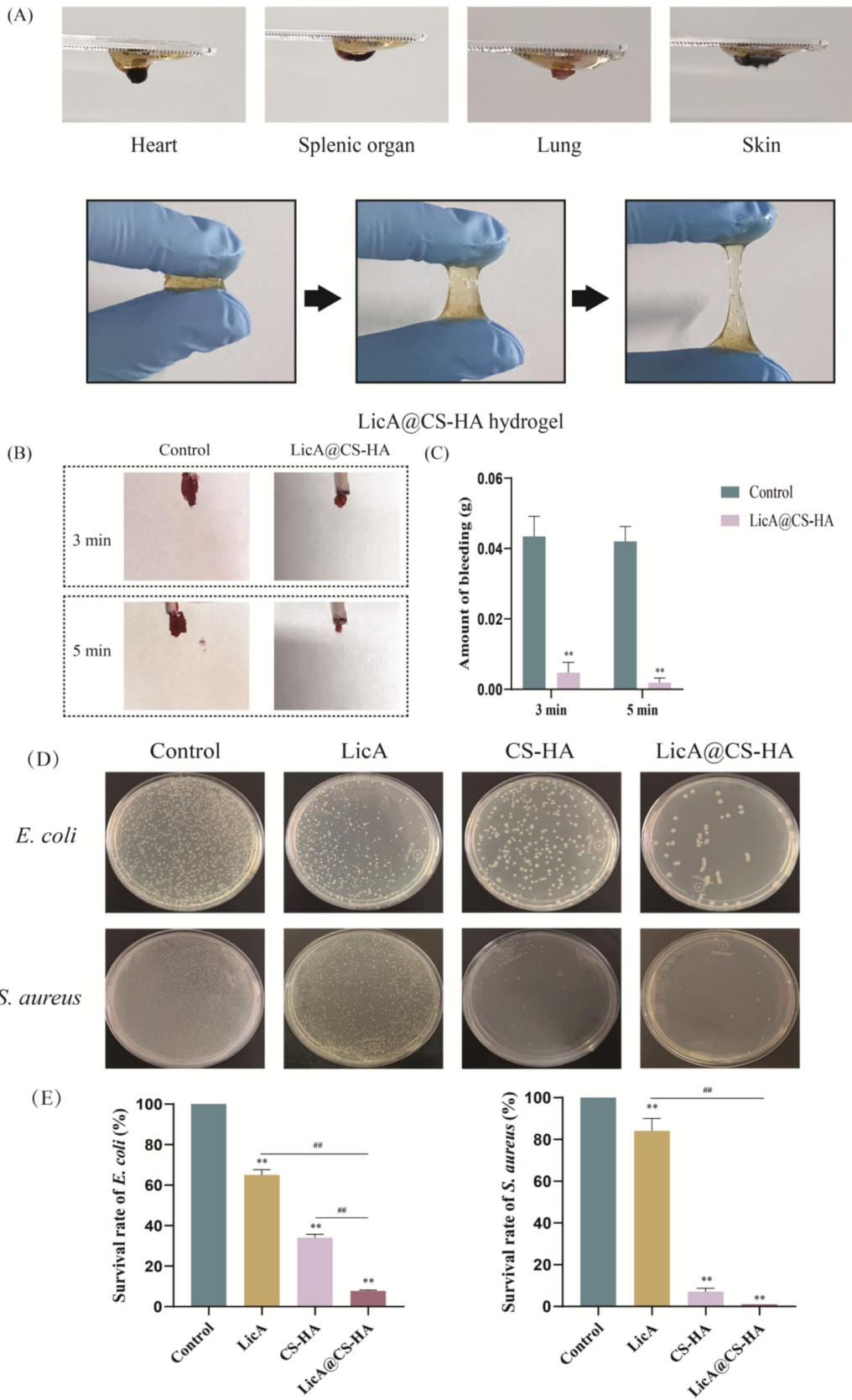
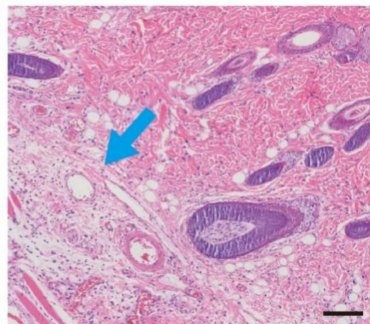
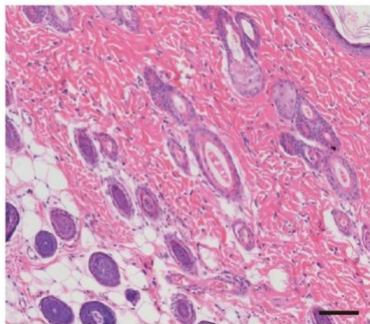


Figure 3AE

(F) Con CS-HA hydrogel

Day 7



Day 14

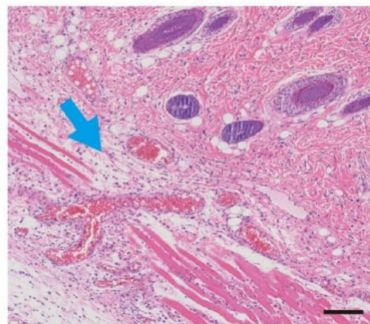
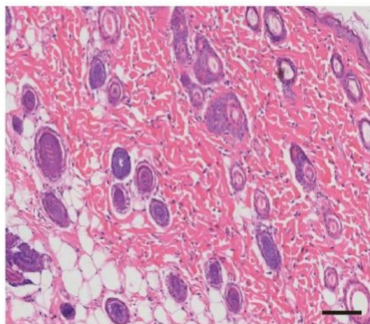


Figure 3F

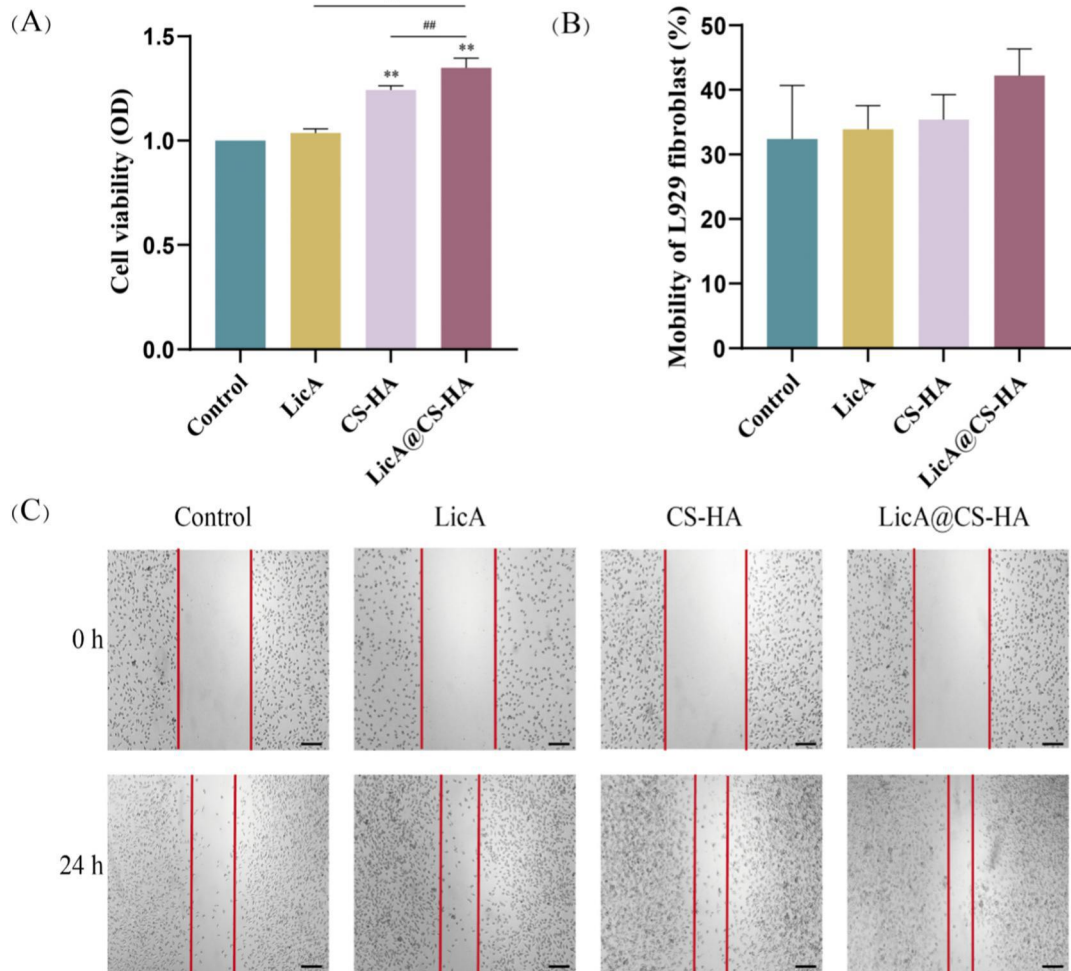


Figure 4

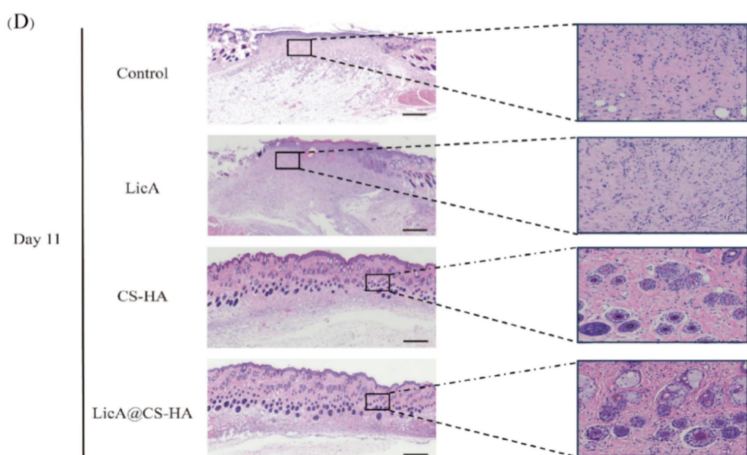
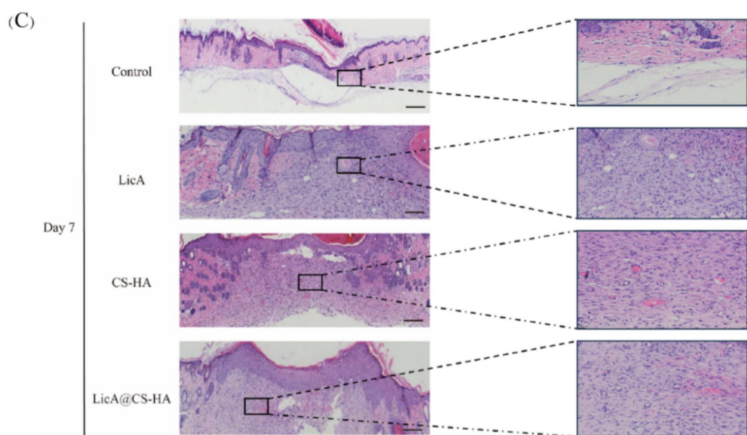
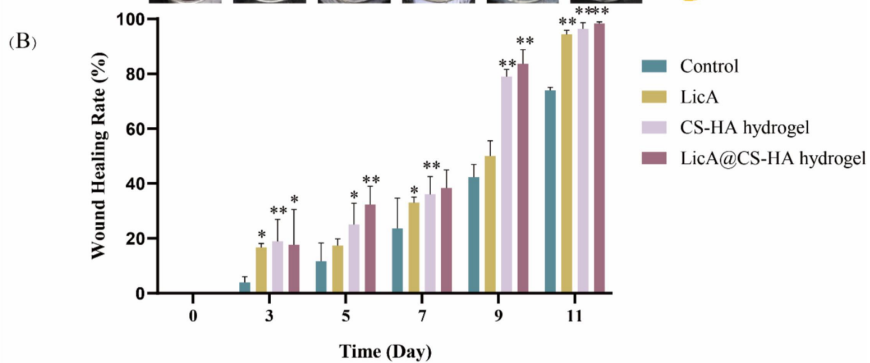
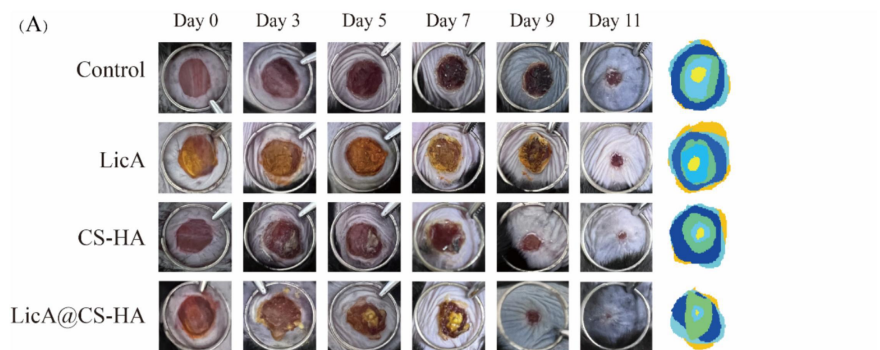
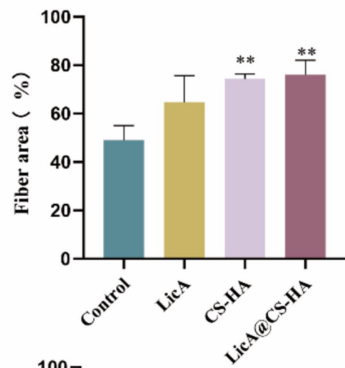
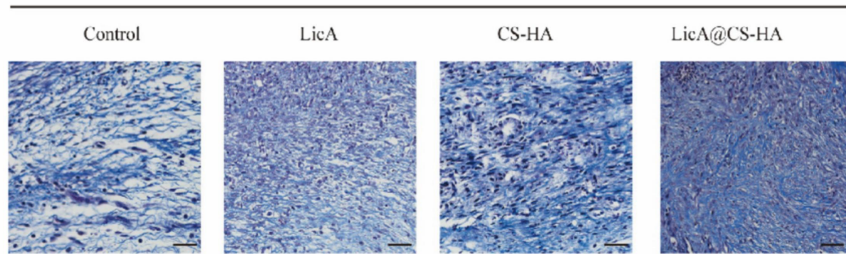


Figure 5AD

(E)

Day 7



(F)

Day 11

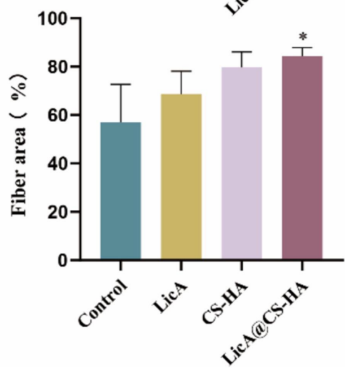
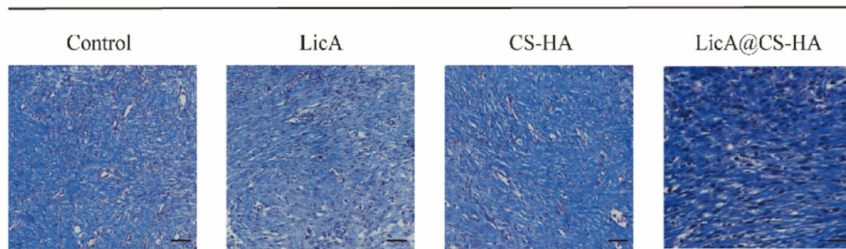


Figure 5EF

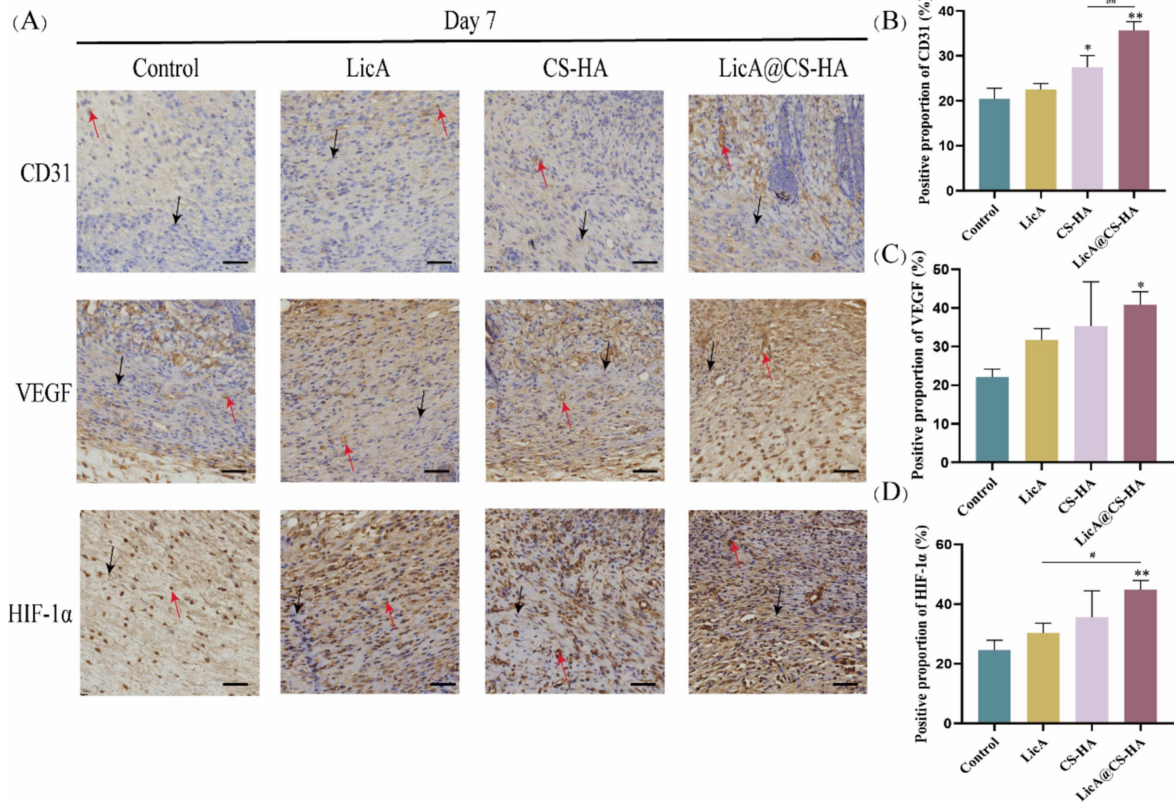


Figure 6

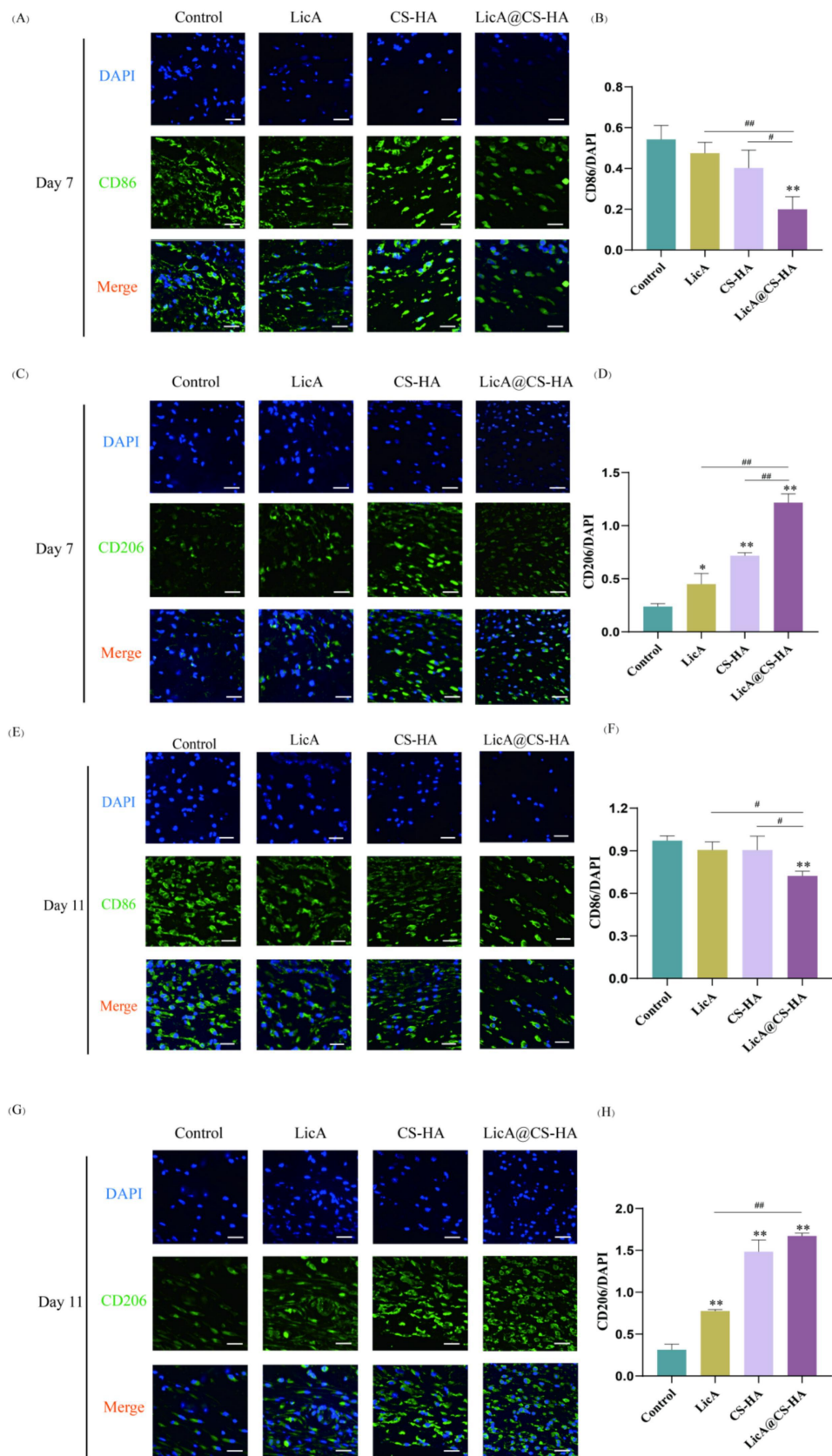


Figure 7

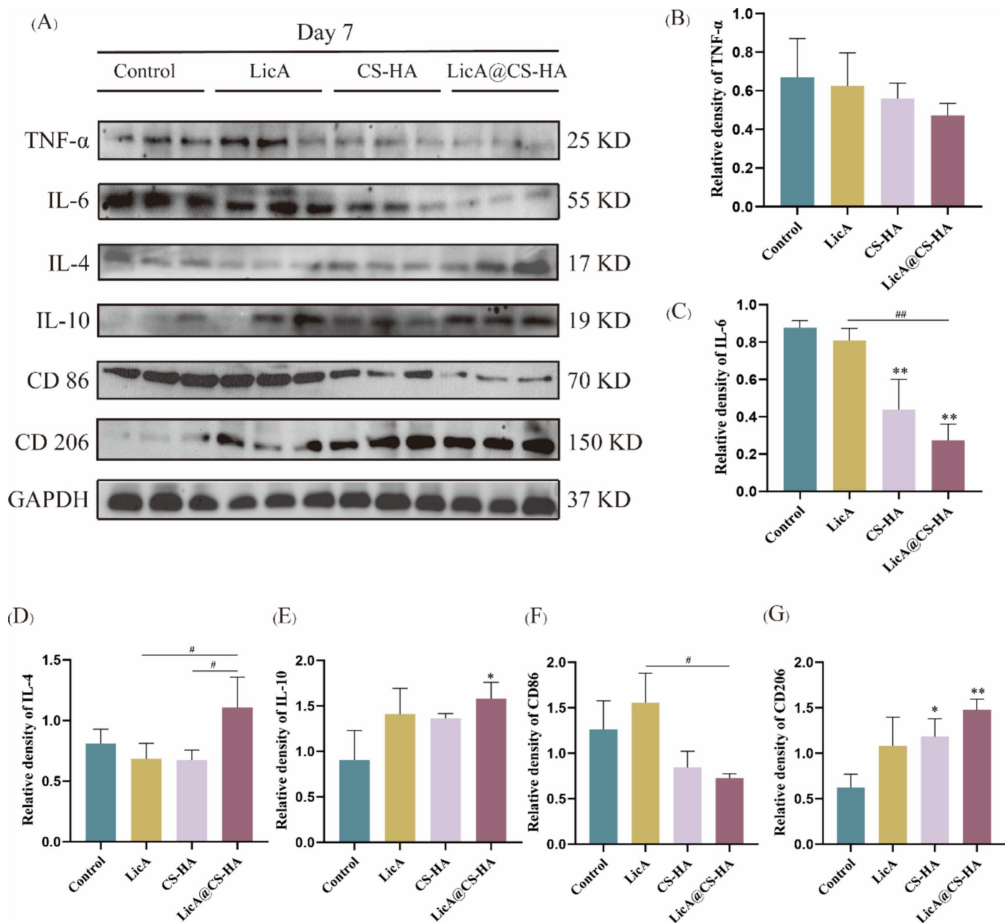


Figure 9